

ANALYTICAL STUDIES OF THE SUSPENDED ZIPPER FRAME & CONTROL DEVICES

K. Denaye Hinds¹ K. Walsh², M. Hill³, M. Abdullah⁴

¹Undergraduate Student & Author ²Assistant Professor & Advisor ³Ph.D. Student ⁴REU Faculty Advisor
Department of Civil & Environmental Engineering, Florida A&M University
Multi-Disciplinary Center for Earthquake Engineering

Abstract

Earthquakes tend to strike suddenly, violently and without ample warning. (FEMA, 2006) The effects of these natural events can be devastating, lead to severe damage; structural failure and potential loss of lives. In the last 20 years, more emphasis has been placed on increasing both the ductility and energy dissipation capability of structures in seismic areas. (Yang, 2006) Seismic control devices and bracing systems are becoming an imperative necessity in the design and mitigation of those structures against earthquakes. As a result there have been many innovations regarding bracing systems. This research involves modeling a suspended zipper frame and its elements, the analytical research of its current structural components, as well as the determination of dynamic structural control systems to be incorporated into the seismic analysis of the zipper frame. An innovative bracing system known as the suspended zipper frame incorporates a design strategy which allows for ductile behavior of a structure. It ensures higher strength than typical bracing systems and can improve the overall seismic performance without utilizing overly stiff beams. The Direct Stiffness Method and Force Method will be utilized in the modeling and analysis of the zipper frame. Passive structural control devices provide additional energy dissipation capability for structures. With the addition of a passive control device, the ability for the suspended zipper frame to optimally reduce its response during seismic loading can be achieved. The passive fluid viscous damper will be modeled using MATLAB computer software and incorporated into the zipper frame model.

Introduction

Although ninety percent of the world's earthquakes occur in regions with major cities, such as Tokyo, Los Angeles and Athens, earthquakes are not uncommon to other parts of the world. In the year 1999, Taiwan suffered an earthquake of magnitude 7.7 on the Richter Scale, which resulted in the death of 2,297 people. In 2004, North Sumatra saw a death toll of 283,106 people after enduring 9.1 magnitude earthquake, and in 2007 the Solomon Islands experienced an earthquake of a 9.1 magnitude proportion. Europe saw seven earthquakes in 2007, Asia suffered a total of 41, Australia had 19, Africa experienced six earthquakes and the United States has seen 111 earthquakes in the year 2007 alone. (USGS, 2007) The identification of mitigation measures can potentially save

lives. Thus there is an increasing need to analyze structures to combat the effects of earthquakes.

The Zipper Frame is an innovative bracing system designed to increase the ductility and stiffness of a system under seismic loading and assist in damage distribution. It utilizes a zipper strut mechanism to support the frame of the system at its mid-span. The mechanism performs at partial height of the system, allowing simultaneous buckling of the braced members on the floors of the system. Due to the partial zipper mechanism, the top floor remains elastic thus increasing the stability of the system.

Fluid Viscous Damper is a passive structural control device which utilizes fluid forces, which are produced by a piston in a hydraulic cylinder, to be pushed through orifices (holes within the cylinder) under high pressure to dissipate energy of a system. The amount of force produced by the control device is dependent on the viscosity of the fluid used within the device as the size of the orifices, which allow the fluid to pass through the device. A schematic of the Fluid Viscous Damper is shown in Figure 1. This passive control is incorporated into the zipper frame to decrease the overall system response given an earthquake event.

The control contributes to the dissipation of energy while the bracing system accounts for the ductility of the system.

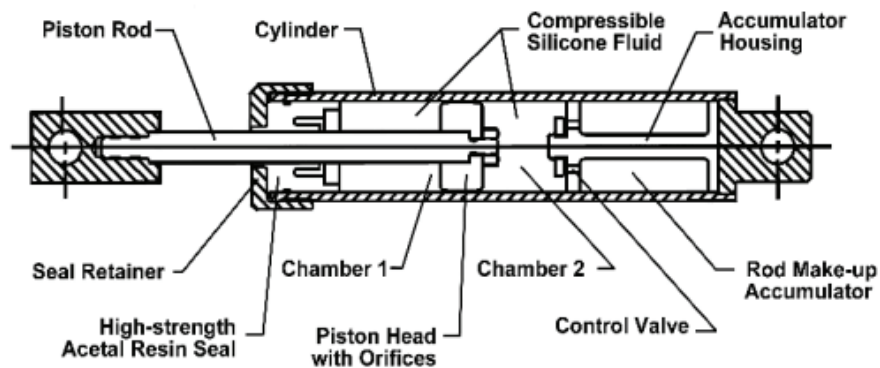


Figure 1: Fluid Viscous Damper Schematic

Bracing Systems

Bracing systems assist in the resistance of lateral forces experienced by structures under seismic activity. The high axial forces which are developed in selected framing members, internal axial actions and relatively small flexural actions, allow for the bracing systems to resist lateral loadings. The ability for braced systems to control frame drift under high earthquake-induced inertial forces contributed to the popularity of its implementation into regions of high seismicity. (Yang, 2006) There are several concentrically braced frame configurations as shown in Figure 2, in this paper we will focus on Inverted V-braced (Chevron Braced) frames depicted in Figure 2b.

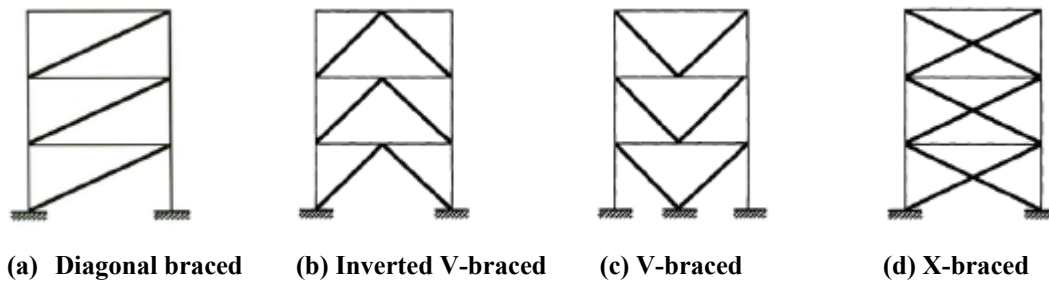


Figure 2: Concentrically Braced Frame Configurations

Concentrically Braced Frames with Chevron Bracing (CBF) – This particular framing system the behavior and response of the system is dictated by the buckling of the first floor brace, which is denoted by the thick line in Figure 3(b). Once the compression brace has buckled, yielding of the first floor occurs resulting in the localization of failure and a loss of lateral resistance as shown in Figure 3(c). The first floor becomes inelastic resulting in collapse of the frame. CBF's exhibit little force re-distribution capabilities are not suitable for resisting earthquake loadings.

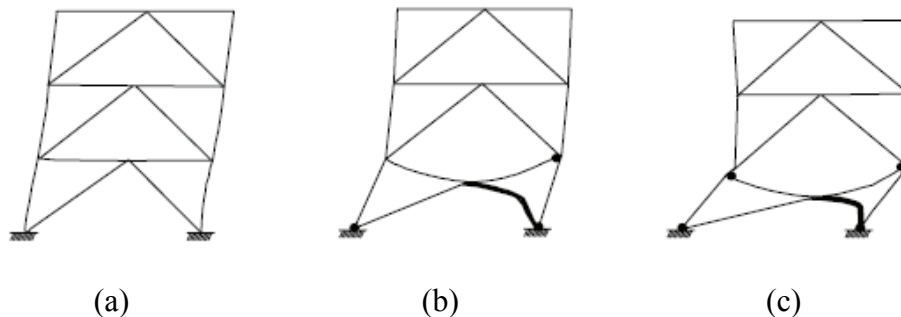


Figure 3: Concentrically Braced Frame w/ Chevron Bracing

Special Concentrically Braced Frames with Special Chevron Bracing and Zipper Struts (SCBF & ZS) – Zipper struts are incorporated into the concentrically braced frame at the mid-span to mobilize stiffness to resist the unbalance of vertical forces sustained once continued lateral displacement occurs within the system. The zipper struts also assist in the resistance of the post-buckling forces experienced by the members due to continuous loading. The concept of the SCBF & ZS is to incur simultaneous buckling of compression members as show in Figure 4(b) and 4(c). However once the buckling of the top floor occurs, the zipper struts are at full zipper mechanism resulting in the top floor of the system becoming in-elastic, Figure 4(d). Under this condition the system loses lateral capacity and failure occurs. To combat this action the beam sizes of the SCBF & ZS would have to be increased; this is not an economical solution.

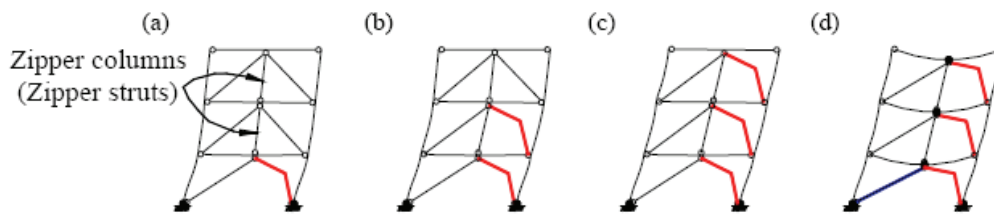


Figure 4: SCBF with SCB and ZS

Control Devices

Structural control devices may be incorporated into a system to assist in the achievement of lower response due to seismic activity. Control devices also contribute to the structural safety and energy dissipation of systems. Control devices include:

Active Control – Active devices have the capability to elevate structural concepts from a static and passive level to a dynamic and adaptable level; thus allowing for the control to dynamically modify the response of a structure in order to increase the safety and reliability. (Lametrie, 2001) However active devices require large power sources to be operational; in the event of a power outage, this control will become rendered useless.

Semi-Active Control – These controls rely on motion of a structure to create control. Semi-active controls also have the ability to alter their properties to produce the appropriate control forces. However the complexities of a semi-active system and the expense of its production and operations leave much to be desired of its use.

Passive Control – Passive controls are the most commonly used structural control device. They rely on the motion of the structure, under seismic loading, to produce a control force. Unlike the active control, passive controls do not need large power sources, thus given the absence of power the device will still be relevant to the control of the building. Passive controls are very inexpensive and less complex than semi-active controls.

Objective

The objective of this research is to incorporate a passive control device into the zipper frame model to increase the energy dissipation and compliment ductility. To successfully accomplish this objective the suspended zipper frame and its elements will be modeled and an analysis of its current structural components will be conducted. The model will be verified by OpenSees software and the responses of both models compared. The response of the system with and without the control device will be compared. The effects of the dynamic control systems to be incorporated into the zipper frame will be determined.

Methodology

Several analytical methods were utilized to generate the desired information need meet the objectives of this research. The first method, Direct Stiffness Method (DSM) was considered in order to determine global stiffness matrix of the zipper frame. Once this had been determined the Force Method (FM) was incorporated to reduce the zipper frame system into a 2DOF lump mass model to allow for less complicated analysis for application of the equations of motion. The zipper frame was then analytically modeled and its response recorded from the 1995 Kobe (LA22) earthquake ground accelerations using the Equations of Motion (EM). A passive control device was then modeled using MATLAB and the zipper frame responses were modeled and compared.

Direct Stiffness Method

DSM is used to directly analyze determinant and indeterminate structures. This method relates the global stiffness, displacements and forces of the entire system to the local stiffness, displacements and forces of each member in the system. It utilizes elements and nodal references to develop a system of coordinates to successfully determine the stiffness matrix for the entire system.

The system is divided into finite elements for which nodes and degrees of freedom (DOF) are established. Each element is denoted by numerical notation outlined in a box. Nodes are denoted by numbers in circles, and the degrees of freedom of each node (three DOF per node) are represented as N_x (horizontal), N_y (vertical) and N_z (rotation), as in Figure 5. This system yields 18 total DOF.

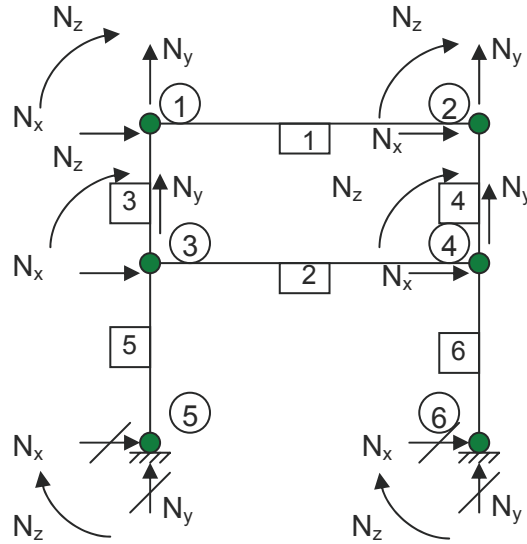


Figure 5: Example 2-Story System Displaying Nodes, Elements & DOF

Once the elements, nodes and degrees of freedom are established for the system, the local stiffness matrix can be developed based on the properties of each element. The local stiffness matrix, \mathbf{k}' is shown in Equation 1.

$$\mathbf{k}' = \begin{bmatrix} \frac{EA}{L} & 0 & 0 & -\frac{EA}{L} & 0 & 0 \\ 0 & \frac{12EI}{L^3} & \frac{6EI}{L^2} & 0 & -\frac{12EI}{L^3} & \frac{6EI}{L^2} \\ 0 & \frac{6EI}{L^2} & \frac{4EI}{L} & 0 & -\frac{6EI}{L^2} & \frac{2EI}{L} \\ -\frac{EA}{L} & 0 & 0 & \frac{EA}{L} & 0 & 0 \\ 0 & -\frac{12EI}{L^3} & -\frac{6EI}{L^2} & 0 & \frac{12EI}{L^3} & -\frac{6EI}{L^2} \\ 0 & \frac{6EI}{L^2} & \frac{12EI}{L^3} & 0 & -\frac{6EI}{L^2} & \frac{4EI}{L} \end{bmatrix} \quad (1)$$

E represents the modulus of elasticity of element, A is the area of element, I represents the moment of inertia and L, the length of element.

Given the local stiffness matrix we are able to convert to the local-global stiffness matrix, which is the local stiffness of each element of the system represented in global coordinates. Equation 2 yields the local-global stiffness matrix.

$$\mathbf{k} = \mathbf{T}^T \mathbf{k}' \mathbf{T} \quad (2)$$

Where, \mathbf{k}' is the local stiffness matrix (Equation 1) and \mathbf{T} is the transformation matrix as denoted in Equation 3.

$$\mathbf{T} = \begin{bmatrix} \lambda_x & \lambda_y & 0 & 0 & 0 & 0 \\ -\lambda_y & \lambda_x & 0 & 0 & 0 & 0 \\ 0 & 0 & 1 & 0 & 0 & 0 \\ 0 & 0 & 0 & \lambda_x & \lambda_y & 0 \\ 0 & 0 & 0 & -\lambda_y & \lambda_x & 0 \\ 0 & 0 & 0 & 0 & 0 & 1 \end{bmatrix} \quad (3)$$

Lambda is based on the coordinates of the near and far nodes of each element, referenced in Figure 6. The general equation for lambda is given by Equations 4 and 5.

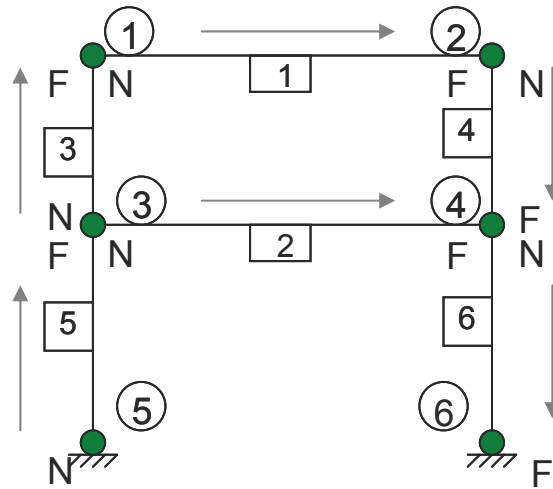


Figure 6: Near & Far References

$$\lambda_x = \frac{x_F - x_N}{L} \quad (4)$$

$$\lambda_y = \frac{y_F - y_N}{L} \quad (5)$$

Where x_N represents the near nodal coordinate along the x-axis, x_F represents the far nodal coordinate along the x-axis; y_F and y_N are the near and far nodal coordinates along the y-axis respectively. L represents the length of the element.

The local-global stiffness matrix is represented in the following matrix.

$$\mathbf{k} = \begin{bmatrix} \left(\frac{AE}{L}\lambda_x^2 + \frac{12EI}{L^3}\lambda_y^2\right) & \left(\frac{AE}{L} - \frac{12EI}{L^3}\right)\lambda_x\lambda_y & -\left(\frac{6EI}{L^2}\lambda_y\right) & -\left(\frac{AE}{L}\lambda_x^2 - \frac{12EI}{L^3}\lambda_y^2\right) & -\left(\frac{AE}{L} - \frac{12EI}{L^3}\right)\lambda_x\lambda_y & -\left(\frac{6EI}{L^2}\lambda_y\right) \\ \left(\frac{AE}{L} - \frac{12EI}{L^3}\right)\lambda_x\lambda_y & \left(\frac{AE}{L}\lambda_y^2 + \frac{12EI}{L^3}\lambda_x^2\right) & \left(\frac{6EI}{L^2}\lambda_x\right) & -\left(\frac{AE}{L} - \frac{12EI}{L^3}\right)\lambda_x\lambda_y & -\left(\frac{AE}{L}\lambda_y^2 + \frac{12EI}{L^3}\lambda_x^2\right) & \left(\frac{6EI}{L^2}\lambda_x\right) \\ -\left(\frac{6EI}{L^2}\lambda_y\right) & \left(\frac{6EI}{L^2}\lambda_x\right) & \left(\frac{4EI}{L}\right) & \left(\frac{6EI}{L^2}\lambda_y\right) & -\left(\frac{6EI}{L^2}\lambda_x\right) & \left(\frac{2EI}{L}\right) \\ -\left(\frac{AE}{L}\lambda_x^2 + \frac{12EI}{L^3}\lambda_y^2\right) & -\left(\frac{AE}{L} - \frac{12EI}{L^3}\right)\lambda_x\lambda_y & \left(\frac{6EI}{L^2}\lambda_y\right) & \left(\frac{AE}{L}\lambda_x^2 + \frac{12EI}{L^3}\lambda_y^2\right) & \left(\frac{AE}{L} - \frac{12EI}{L^3}\right)\lambda_x\lambda_y & \left(\frac{6EI}{L^2}\lambda_y\right) \\ -\left(\frac{AE}{L} - \frac{12EI}{L^3}\right)\lambda_x\lambda_y & -\left(\frac{AE}{L}\lambda_y^2 + \frac{12EI}{L^3}\lambda_x^2\right) & -\left(\frac{6EI}{L^2}\lambda_x\right) & \left(\frac{AE}{L} - \frac{12EI}{L^3}\right)\lambda_x\lambda_y & \left(\frac{AE}{L}\lambda_y^2 + \frac{12EI}{L^3}\lambda_x^2\right) & -\left(\frac{6EI}{L^2}\lambda_x\right) \\ -\left(\frac{6EI}{L^2}\lambda_y\right) & \left(\frac{6EI}{L^2}\lambda_x\right) & \left(\frac{2EI}{L}\right) & \left(\frac{6EI}{L^2}\lambda_y\right) & -\left(\frac{6EI}{L^2}\lambda_x\right) & \left(\frac{4EI}{L}\right) \end{bmatrix}$$

The global stiffness matrix, \mathbf{K} , depends on the collective placement of all \mathbf{k} matrices, based on the common DOF of each element. The size of \mathbf{K} is dependent on the total DOF of the system, thus given the 2-story example figure, the global matrix \mathbf{K} , will be an [18x18] matrix.

Force Method

The force method assumes that the entire mass of the system is concentrated at each floor of the system. It also assumes that the average displacement of each floor occurs in one direction, horizontal. A unit horizontal force, less than or equal to one, is applied at each floor separately and the displacement of each floor relevant to the force is calculated. Consider the 2-story example in Figure 7.

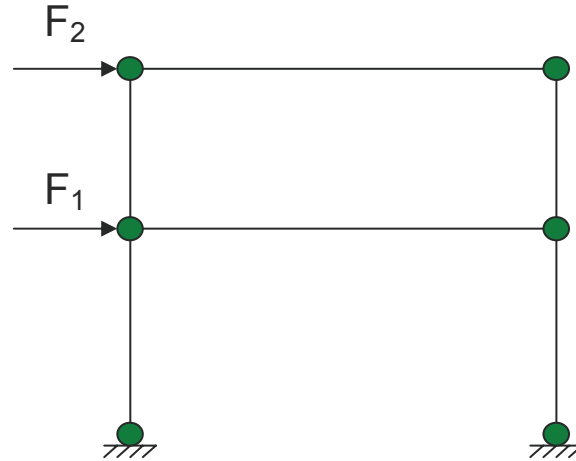


Figure 7: Example 2-story system with applied unit loading

The displacements of floors one and two with respects to F_1 are calculated, yielding δ_{11} and δ_{21} . F_1 is removed and F_2 is applied to the system. The displacements of floors, one and two, with respects to F_2 are then calculated, yielding δ_{12} and δ_{22} . The flexibility matrix, δ is constituted, shown by Equation 7.

$$\delta = \begin{bmatrix} \delta_{11} & \delta_{12} \\ \delta_{21} & \delta_{22} \end{bmatrix} \quad (7)$$

From the flexibility matrix the lump stiffness, \mathbf{K}_{LM} , is determined via Equation 8.

$$\mathbf{K}_{LM} = \delta^{-1} \quad (8)$$

The example 2-story system can now be represented as a 2-DOF lump mass model, shown in Figure 8, to allow for simplified analysis. The mass of the system is represented by M_1 and M_2 lumped at each floor and the stiffness K_{LM1} and K_{LM2} are the stiffness between each floor of the system.

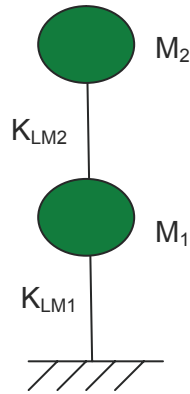


Figure 8: Example 2-DOF Lump Mass Model

Equations of Motion

The equations of motion are used to model the dynamics of a system. The system properties which are modeled consist of the displacements, velocities and accelerations. Each of these is modeled with respects to ground motion to calculate the response of the system. Every system has mass; weight of the system, stiffness; the ratio of applied force to deformation and damping; ability to dissipate energy; these properties are related by the governing equation of motion given in Equation 9. The left side of the equation represents the inputs, mass, acceleration, damping, velocity, stiffness and displacements all with respect to time. The right side of the equation represents the output, earthquake forces and the structural control forces.

$$\mathbf{M}\ddot{\mathbf{x}}(t) + \mathbf{C}\dot{\mathbf{x}}(t) + \mathbf{K}\mathbf{x}(t) = \mathbf{E}\mathbf{F}_e(t) + \mathbf{H}\mathbf{F}_c(t) \quad (9)$$

where:

\mathbf{M} = nxn diagonal mass matrix

\mathbf{C} = nxn symmetric damping matrix

\mathbf{K} = nxn symmetric stiffness matrix

$\ddot{\mathbf{x}}$ = nx1 acceleration vector

$\dot{\mathbf{x}}$ = nx1 velocity vector

\mathbf{x} = nx1 displacement vector

\mathbf{E} = nxr earthquake location matrix

\mathbf{F}_e = nx1 earthquake vector

\mathbf{H} = nxm control force location matrix

\mathbf{F}_c = mx1 control vector

n = number of floors

m = number of control devices

r = number of earthquake inputs

By representing the governing equation as a state-space equation, we can simplify the second order governing equation to a first order equation by, given in Equation 10.

$$\dot{\mathbf{z}}(t) = \mathbf{A}\mathbf{z}(t) + \mathbf{B}\mathbf{u}(t) \quad (10)$$

\mathbf{A} is a system properties matrix, \mathbf{z} is the states of the system vector (displacement and velocity) with respects to time, \mathbf{B} is the control force location matrix, \mathbf{u} is the earthquake and control force vectors and $\dot{\mathbf{z}}$ is the derivative of the states of the system (velocity and acceleration) vector. The matrix and vector representation of the state space equation is expressed in the following equation.

$$\begin{bmatrix} \dot{\mathbf{z}}_1 \\ \dot{\mathbf{z}}_2 \end{bmatrix} = \begin{bmatrix} \dot{\mathbf{x}}(t) \\ \ddot{\mathbf{x}}(t) \end{bmatrix} = \begin{bmatrix} \mathbf{0}_{(n \times n)} & \mathbf{I}_{(n \times n)} \\ -\mathbf{M}^{-1}\mathbf{K}_{(n \times n)} & -\mathbf{M}^{-1}\mathbf{C}_{(n \times n)} \end{bmatrix} \begin{bmatrix} \mathbf{x}_{(n \times 1)} \\ \dot{\mathbf{x}}_{(n \times 1)} \end{bmatrix} + \begin{bmatrix} \mathbf{0}_{(n \times r)} & \mathbf{0}_{(n \times m)} \\ \mathbf{M}^{-1}\mathbf{E}_{(n \times r)} & \mathbf{M}^{-1}\mathbf{H}_{(n \times m)} \end{bmatrix} \begin{bmatrix} \mathbf{F}_e(r \times 1) \\ \mathbf{F}_c(m \times 1) \end{bmatrix}$$

Derivative of states
Properties of system matrix, \mathbf{A}
States of system, \mathbf{z}
Location matrix, \mathbf{B}
External input, \mathbf{u}

Fluid Viscous Damper

Fluid Viscous Dampers, with much success, utilize forces generated by surface friction to dissipate vibratory energy in a structural system. Their ability to reduce drifts within multi-story seismically excited buildings has been employed in conjunction with seismic isolation systems. (Lametrie, 2001) Such a system has proven to be effective and can be mathematically analyzed using algorithms and linear algebra.

Recall the equation of motion, Equation 9 and the state space representations, Equations 10 and 11. F_c (Equation 9 and 11) and $\mathbf{u}(t)$ in Equation 10 refers to the control force. The fluid viscous damper is modeled to determine the control force and damping coefficient for the system to enable sufficient control of the system given an earthquake. The control force equation is given by Equation 12.

$$F_C(t) = C_D \dot{\mathbf{x}}_{\text{piston}}(t) \quad (12)$$

Where $F_c(t)$ is equal to the force of the damper with respect to time, C_D represents the damping of the device and $\dot{x}_{\text{piston}}(t)$ is the velocity of the piston, with respect to time.

The damping coefficient, C_D is calculated using Equation 13, derived by Consantnou and Symans.

$$C_{D_i} = \frac{4\pi\xi_j \sum_i^n m_i \Phi_{i,j}^2}{T_j \sum_i^n (\Phi_{i,j} - \Phi_{i,j})^2} \quad (13)$$

ξ = damping ratio

m_i = mass

$\Phi_{i,j}$ = mode

T_j = period

i = floor number

n = number of floors

j = mode of vibration

The Zipper Frame

The zipper frame is a three story, fixed connection, concentrically braced framing system, with fixed end supports, which incorporates chevron bracing and suspended zipper columns at its mid-span. It is comprised of ASTM A500 Grade B Steel with an ultimate tensile strength of 58ksi and a flexural buckling compressive strength of 40.5ksi and 43.5ksi for the bottom two floors and top floor respectively. The frame consists of twenty elements overall, six beams, six columns, six braces, and two zipper columns, each shown in Figure 9. The member properties of the zipper frame are expressed in Table 1.

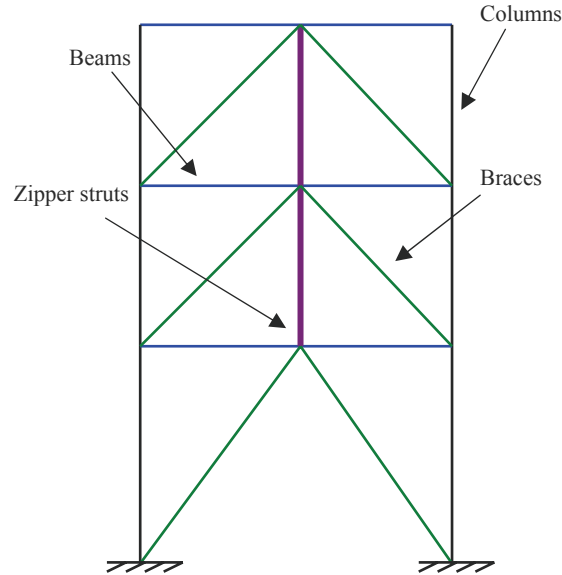


Figure 9: Zipper Frame

Table 1: Zipper Frame Member Properties

Floor	Braces	Columns	Beams	Zipper Struts
1	<i>HSS 2x2x1/8</i>	<i>S 4x9.5</i>	<i>S 3x7.5</i>	
	A = 0.84 in ²	A = 2.79 in ²	A = 2.20 in ²	
	I = 0.486 in ⁴	I = 0.887 in ⁴	I = 2.91 in ⁴	
	L = 65.6 in	L = 52 in	L = 40 in	
2	<i>HSS 2x2x1/8</i>	<i>S 4x9.5</i>	<i>S 5x10</i>	<i>HSS 1.25x1.25x3/16</i>
	A = 0.84 in ²	A = 2.79 in ²	A = 2.93 in ²	A = 0.67 in ²
	I = 0.486 in ⁴	I = 0.887 in ⁴	I = 12.3 in ⁴	I = 0.12 in ⁴
	L = 65.6 in	L = 52 in	L = 40 in	L = 52 in
3	<i>HSS 3x3x3/16</i>	<i>S 4x9.5</i>	<i>S 3x5.7</i>	<i>HSS 2x2x3/16</i>
	A = 1.89 in ²	A = 2.79 in ²	A = 1.66 in ²	A = 1.19 in ²
	I = 2.46 in ⁴	I = 0.887 in ⁴	I = 2.50 in ⁴	I = 0.641 in ⁴
	L = 65.6 in	L = 52 in	L = 40 in	L = 2 in

Given the member properties and configuration, the zipper frame the zipper frame was modeled and the stresses of each brace member calculated to determine the stress distribution of each brace with respects their order of failure. The mechanism of the zipper frame is to incur a stress distribution which allows for the buckling of the first story braces, increase the stress distribution from the first floor to the second floor and then achieve buckling of the second story braces. By modeling the zipper frame in MATLAB and solving for the stresses of each braced member we are able to observe the pattern of stress distribution.

Results & Comparisons

Model Verification

The zipper frame modeled in MATLAB was verified by the comparison of the properties determined by Yang. The zipper frame was also modeled using OpenSees software, the results obtained were compared to those from MATLAB and contributed to the verification of the model and its properties.

The structural periods of a system describe its ability to vibrate based on inherent properties within the system. The following Table gives the comparison of the periods of each floor for MATLAB and OpenSees.

Table 2: Structural Periods

	MATLAB	OpenSees
1 st Floor	0.50	0.34
2 nd Floor	0.16	0.11
3 rd Floor	0.10	0.07

Mode Shapes describe a structures movement with respects to its frequencies. Therefore at any given frequency there is a way to observe the vibration of the structure. The following figures describe the first three mode shapes of the zipper frame. Figure 10 depicts the mode shapes which were determined via MATLAB software using eign-value analysis. It is clear to see the similarities in the modes shapes of Figure 10 with respects to those in Figure 11, found by Opensees. The first and second floor modes are considerably close in comparison, while the third floor is slightly off; there is still verification in the ability to replicate the mode shapes of the zipper frame structure.

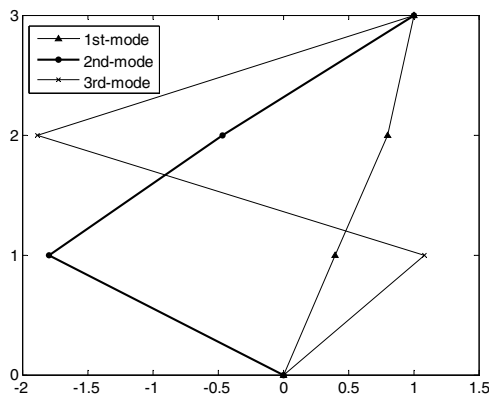


Figure 10: MATLAB, Mode Shapes

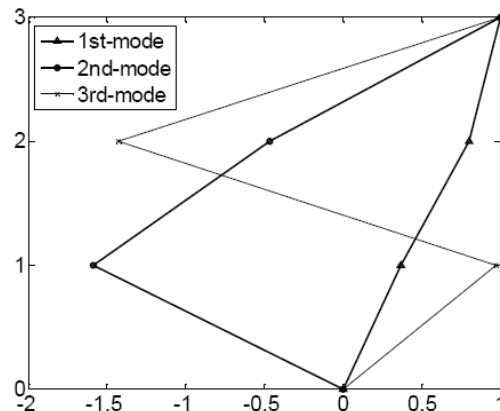


Figure 11: OpenSees, Mode Shapes

The displacements and accelerations for the uncontrolled case of each floor of the zipper frame given earthquake data from the LA22 earthquake are displayed in the following Table. The data calculated from MATLAB and OpenSees software are compared in the Table 3.

Table 3: Displacement & Acceleration Comparison

Floor	Displacements (in)		Accelerations (in/s ²)	
	MATLAB	OpenSees	MATLAB	OpenSees
1	2.4	2.0	368.8	376.1
2	4.8	4.8	811.3	409.1
3	5.8	5.0	1032.5	438.8

The compressive buckling failure of the braced members for the uncontrolled case in the zipper frame can be viewed in the following figures. Many of the braced members reach compressive buckling between 6 to 8 seconds at 40.56ksi. The following figures depict the stress distribution for the entire earthquake and then focus in on the first ten seconds of the earthquake to evaluate the time of buckling of the first floor braced members.

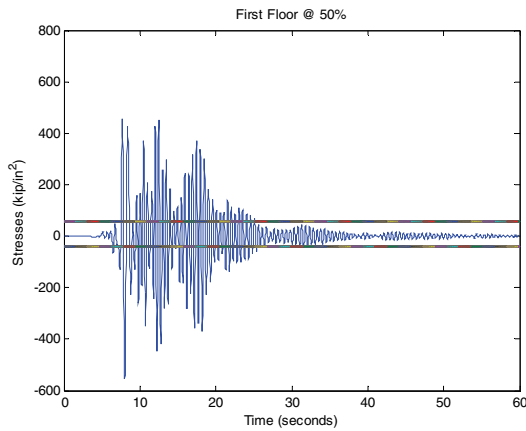


Figure 12: MATLAB Stress Distribution

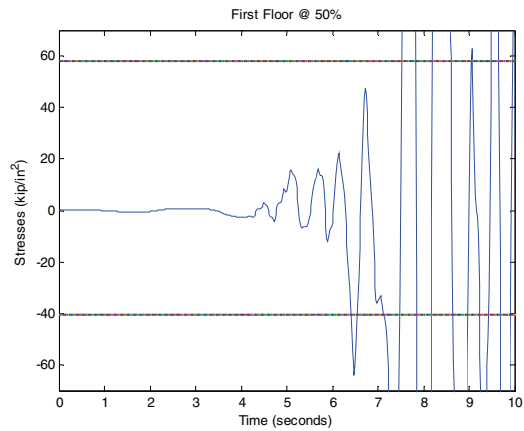


Figure 13: MATLAB Failure Time-point

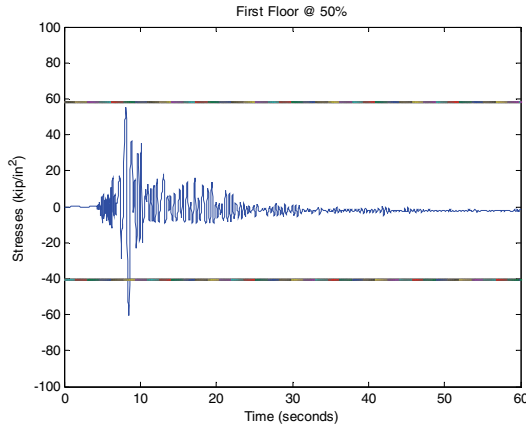


Figure 14: OpenSees Stress Distribution

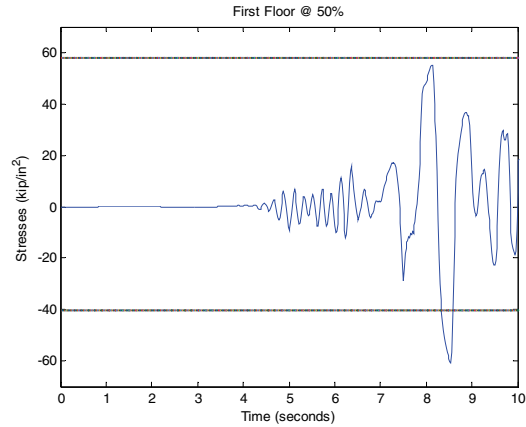


Figure 15: OpenSees Failure Time-point

The time at which the first floor braces buckle are depicted in Table 4. Both models fail within a ten second period and the times at which they fail are close to one another to further verify the modeling of the zipper frame in MATLAB.

Table 4: Time of Buckling Failure – Uncontrolled Cases

Time (s) of Buckling of 1 st Floor	
MATLAB	OpenSees
6.41	8.33

Controlled versus Uncontrolled

The passive fluid viscous damper was incorporated into the zipper frame and the displacements, accelerations and stress distributions were modeled mathematically to determine the effect of the control on the response of the zipper frame. The following graphs represent the displacements of the floors relative to the LA22 ground motions. The graphs represent the case where a damper is placed on second floor and a damper placed on all three floors with both having a damping ratio of 40%. The numerical representations of the displacements given other damper configurations (placements) are given in Table 5. The two best configurations were compared and the percent reductions calculated.

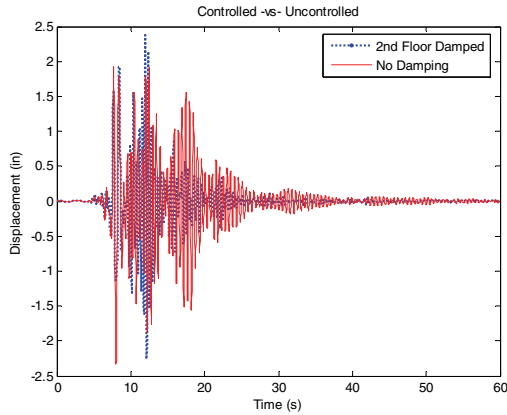


Figure 16: Damper Placed on 2nd Floor

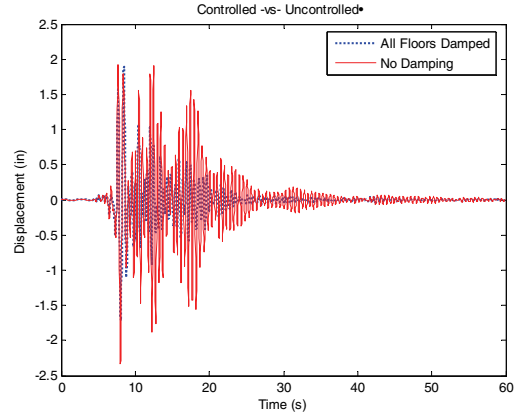


Figure 17: Damper Placed on All Floors

Table 5: Percent Reductions in Displacements (in.) - Damping Configurations -vs- Uncontrolled

Floor	Damper Placement			
	1 st Floor Only	2 nd Floor Only	3 rd Floor Only	All 3 Floors
1 st Floor	12.5	0	4.2	25
2 nd Floor	16.6	43.8	8.3	25
3 rd Floor	5.5	39.7	6.9	25.9

The effects of the damper configurations on the accelerations of the frame were also determined and are displayed in Table 6.

Table 6: Percent Reductions in Accelerations (in/s²) - Damping Configurations -vs- Uncontrolled

Floor	Damper Placement			
	1 st Floor Only	2 nd Floor Only	3 rd Floor Only	All 3 Floors
1 st Floor	-22.3	-70.4	26.5	-24.8
2 nd Floor	24.2	21.6	16.8	30.8
3 rd Floor	30.8	19.3	24.5	40.8

The stress distributions for the controlled second floor damped and all floors damped compared with the uncontrolled no damping cases of the first floor of the zipper frame are graphically represented in Figures 18 through 19. The remaining damper configurations are summarized in Table 7.

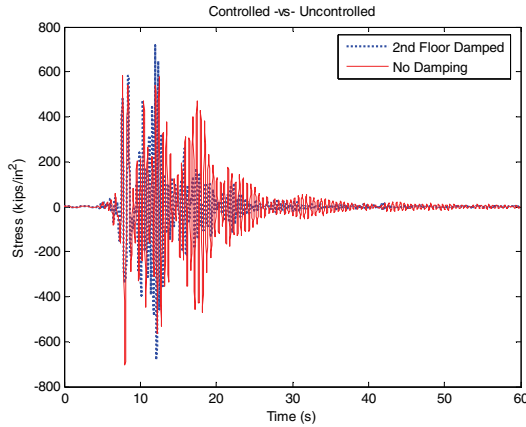


Figure 18: Controlled - 2nd Floor Damped

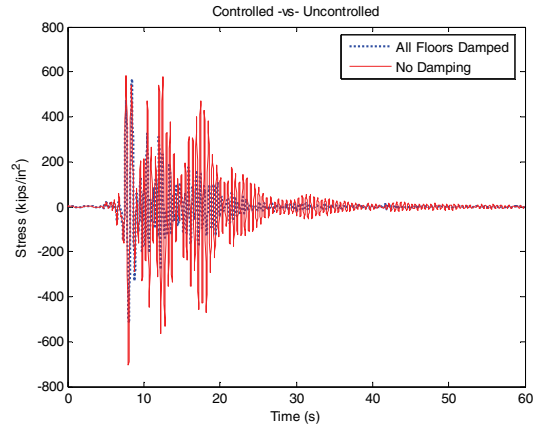


Figure 19: Uncontrolled – No Damping

Table 7: Maximum Compressive Stress (kips/in²)

Floor	Damper Placement				
	Uncontrolled	1 st Floor Only	2 nd Floor Only	3 rd Floor Only	All 3 Floors
1 st Floor	702.8	623.9	679.7	682.3	517.8
2 nd Floor	672.4	592.8	179.4	649.8	473.0
3 rd Floor	336.5	294.8	232.0	319.9	232.0

Conclusions

The verification of the MATLAB model to the OpenSees model yielded very comparable results. The differences in the structural period can be attributed to the method by which the stiffness matrices for the members of the zipper frame were calculated. The specific method by which OpenSees calculates the stiffness differs from the direct stiffness method used. The differences in the acceleration data can be attributed to the fact that MATLAB is a linear, elastic modeling software, whereas OpenSees is non-linear, inelastic modeling software. Instead of a member releasing energy once the limit states are reached through elastic modeling it absorbs energy allowing an increase in acceleration of the system. The mode shapes and displacements calculated using MATLAB, when compared to OpenSees, present very strong resemblances, thus verifying that the zipper frame was modeled correctly.

The addition of the passive control improved the overall response of the system. Considering the four damper configurations modeled, placing the control on the second floor and then on all floors yielded the best results in terms of minimizing the overall responses of the zipper frame when subjected to seismic loading. However the stress distributions due to the placement of the passive control on the second floor seems to have altered the zipper mechanism. Thus suggesting that the addition of a control device into the zipper frame has effects on the way in which the frame is predicted to perform.

Future Work

Future work to be considered regarding the research of the zipper frame will be to look at the effects of post-yielding stiffness on the members of and determine the effects of them on the zipper frame mechanism. Also to model the effects of incorporating a semi-active control device into the zipper frame.

Acknowledgements

I would like to acknowledge and thank the MCEER REU program for the sponsorship of this research. This has been a great opportunity and I feel that I have grown and learned a great deal throughout this, my second, undergraduate research experience. I thank Dr. Kenneth K. Walsh, my research professor & advisor, for his dedication and in-depth knowledge of structural dynamics; he made this opportunity a reality. Thank you for sticking with me throughout it all, taking the time to guide and advise me, and for the opportunity to research such a wonderful topic. I appreciate your attention to detail and rigorous research schedules which I was made to stick to, it has made me a better researcher because of it. To Marlon D. Hill, my Ph.D. student mentor, thank you for your encouragement. Aaron Williams, I appreciate your spirit and friendship. A huge thank you to Dr. Makola Abdullah for starting me on this path and allowing me to become a part of this wonderful lab which is doing great work and will continue to produce excellent researchers and research topics. I would like to thank my mother, family and friends for supporting me throughout my academic career and pushing me to always strive for excellence. To the newer members of the lab, Kyle Cronin, Karl Green, Gustavo Munoz and Troy Sneed, you all made work a fun place to be this summer.

Works Cited

Chowdhury, Indrajit, Computation of Rayleigh Damping Coefficients for Large Systems.

Hibbler, Russel, Structural Analysis, Prentice Hall, May 2005

Lametrie, Christine W., A Literary Review of Structural Control: Earthquake Forces, July, 2001.

Qu, W.L., et al. Dynamic Analysis of Wind-Excited Truss Tower with Friction Dampers, July, 2001.

Xu, Y.L., et al. Seismic Response Control of Frame Structures Using Dampers, 2000.

Yang, Chauang-Sheng, Analytical and Experimental Study of Concentrically Braced Frames with Zipper Struts, December, 2006.